The SPEX Speaker

Vol. XI—No. 4 December, 1966

SPEX INDUSTRIES, INC. · 3880 PARK AVENUE · METUCHEN, N. J. 08841 · ☎ (201)-549-7144

RAMAN SPECTROSCOPY REVISITED

By PROF. ALFONS WEBER

Fordham University, New York, N. Y. 10458

ATTESTING to the significance accorded it by the scientific community upon its discovery in 1928 (1), the Raman effect spawned hundreds of papers per year during the 1930s. From the beginning, its primary application was the investigation of molecular structure. Here the gleanings from both infrared and Raman spectra could be collated to complement and confirm each other. The hitch was soon found to be the painstaking care demanded by the seemingly simple Raman phenomenon for new and useful information to be extracted. For unlike absorption and emission spectra—strong, first order effects—Raman spectra are distressingly weak, depending on light scattering, a second order interaction of electromagnetic radiation with matter.

Besides being of considerable value in molecular structure studies, Raman spectroscopy has decided advantages in qualitative and quantitative spectrochemical analysis. Until the advent of the laser, however, experimental difficulties limited this analytical tool to only the most elite industrial laboratories. A comprehensive treatment, written by J. Brandmüller and H. Moser (2) summarizes the field in all its various aspects up to nearly 1960.

Early researchers relied extensively on liquids in their quest for Raman data; gases and solids were found particularly difficult to work with. Reports on O_2, N_2, CO_2 CH_4, C_2H_6, HCl, H_2, D_2, F_2 by Wood, Amaldi, Rasetti, Houston, and Bhagavantam and others served mostly to provide critical data for the development and verification of Raman effect theory, which was presented in conclusive form in 1934 (3). Except for the work of Nielsen and Ward (4) and Cabannes and Rousset (5), gases were neglected until the early 1950s when improved light sources and Raman tube optical systems aroused renewed interest (6, 7, 8). Even then the experimental efforts that had to be made to pursue this research discouraged all but a staunch few who actively engaged in high resolution Raman spectroscopy of gases: H. L. Welsh at the Univ. of Toronto; B. P. Stoicheff, then at the National Research Council of Canada; V. I. Tyulin at the Univ. of Moscow, U. S. S. R.; and this author.

To the rescue in this struggle for meaningful data have come today's laser light sources (9) whose unique properties for generating Raman spectra have essentially retired all natural (i.e., incoherent) sources of radiation no matter what is being studied (gas, liquid or solid) or what the goal (molecular structure, chemical analysis or crystal structure).

The most widely known aspect of Raman spectroscopy is that it enables the study of vibrational and rotational spectra of molecules from which one infers their structure, geometric shape as well as values for bond lengths and interbond angles. Furthermore, the spectrum yields information concerning inter molecular forces such as force, anharmonicity, and centrifugal distortion constants as well as Coriolis coupling coefficients which describe the interactions between vibration and rotation. In all these respects Raman and infrared methods are similar but the different selection rules governing Raman scattering phenomena and absorption phenomena make the two techniques and results obtainable with them complementary to each other. With respect to infrared spectroscopy the Raman effect offers the following enticements:

1) Raman spectra are observed in the visible and ultraviolet where many atomic lines suitable for wavelength and intensity calibration are accessible. (To facilitate measurements, hollow cathode and electrodeless discharge iron and thorium lamps are excellent sources of wavelength standards.)

2) Since water absorbs strongly over much of the infrared spectrum, special precautions must be taken to eliminate or at least minimize its effect otherwise important features of the spectrum under study are either partially obscured or completely masked. But the Raman spectrum of water is obligingly weak and hardly ever interferes.

3) The intensity of Raman bands varies nearly linearly with concentration, making for ease of quantitative analyses. Even for a non-linear intensity-concentration relationship, calibrating curves quickly provide conversions for a photoelectric recording spectrometer.

4) Since molecular rotation-vibration spectra lie in the region from 50 - 4000 cm^{-1} a single recording of Raman shifts covers the whole range. Several sets of prisms or gratings are needed, however, to record the same region of infrared spectra.

5) Pure rotational transitions of polyatomic molecules are readily observed as the rotational Raman spectrum, especially for molecules which do not possess a permanent dipole moment.

6) Selection rules for the Raman effect are more liberal than those for infrared absorption. Consequently, a rotational-vibrational Raman band may offer direct evaluation of molecular parameters whereas the same transition, observed as an infrared band, allows only determination of combinations of these same quantities. Furthermore, because of the difference in selection rules, perturbations may be uncovered which might otherwise remain undetected from infrared data alone.

Some of the disadvantages of Raman spectroscopy are:

1) Colored samples absorb the exciting radiation. One is thus forced to work with a lower, less desirable excitation frequency.

2) Solid and liquid samples must be perfectly clear or Tyndall scattering by the contained impurities mask the weak Raman spectrum.

3) The sample must not fluoresce. If it absorbs the excitation radiation and fluoresces, no Raman spectrum will result. If the incident radiation is not monochromatic and includes frequencies at which the sample fluoresces, the fluorescence spectrum from the unwanted components in the incident radiation may be stronger than the Raman spectrum produced by the primary component (i.e., the exciting line of the Raman effect).

4) Because of the weakness of the effect several tens of hours are required to photograph a spectrum. under high resolution and dispersion, to study rotational and rotational-vibrational Raman spectra of gases. Even the more strongly scattering liquid systems need several-hour exposures. The development of photoelectric Raman spectrometers, however, has overcome this disadvantage for low to medium resolution work.

5) Careful filtering of the incident radiation is important to prevent photodecomposition of the sample.

6) For high-resolution studies of rotational and rotational-vibrational bands high-resolving-power grating spectrographs of low speed best resolve the fine details. Comparable studies are more easily made in the infrared where a lower instrumental resolving power can provide the same limiting resolution.

These difficulties encountered in Raman spectroscopy are, however, largely dispelled when a laser light source provides the exciting radiation. Benefits derived from laser sources compared with any natural (i.e., incoherent) light source such as the well known low pressure mercury arc include:

1) Emission from a laser source consists primarily of coherent "laser radiation" which is highly monochromatic. Although its output also contains incoherent, non-lasing radiations, these are easily filtered out of the beam thus preventing fluorescence or photodecomposition of the sample.

2) Radiation emitted by a neutral atom laser (i.e., He-Ne) or ion laser (i.e., noble gases Ar, Kr, Xe) has a smaller half-width than the 4358A radiation (0.20 cm^{-1}) produced by a water-cooled low-pressure mercury arc. While this smaller half-width (0.15 cm^{-1} for the ion lasers, less than 0.05 cm^{-1} for the 6328A He-Ne line) has little bearing in the investigation of liquids, it is essential in high-resolution Raman spectroscopy of gases and perhaps even of crystals.

3) The high degree of collimation of a laser beam simplifies experimentation since the light source need not be in the immediate proximity of the sample under study.

4) The coherence of laser radiation, already manifest in narrow line width and beam collimation, allows for concentration by simple focusing of all the radiant flux into a diffraction-limited volume to accommodate microsamples of less than 10^{-7} liters (10^{-4}cc).

5) Commonly, He-Ne and noble gas ion lasers are equipped with plasma tubes sealed with Brewster angle windows. Such laser radiation is nearly 100% linearly polarized and the state of polarization of the well collimated beam can be exploited to considerable advantage in the determination of depolarization factors of Raman lines. It also offers a unique means of conducting precision intensity measurements and assigning Raman spectra of crystals. Furthermore, the very strong Rayleigh scattering of the exciting radiation can be at least partially suppressed by observing the scattered radiation in a direction parallel to that of vibration of the electric vector of the laser radiation.

6) Exciting frequencies may be chosen to suit a specific problem. With a noble gas ion laser refillable with Ar, Kr, or Xe, dozens of lines are available from 4500A to 1μ. Even without changing the gas different lines can be utilized simply by adjusting a wavelength selector prism that is part of the laser cavity.

Thus, not only have today's Raman spectroscopy studies been enhanced by the introduction of laser sources; experiments previously considered impossible now beckon for attention.

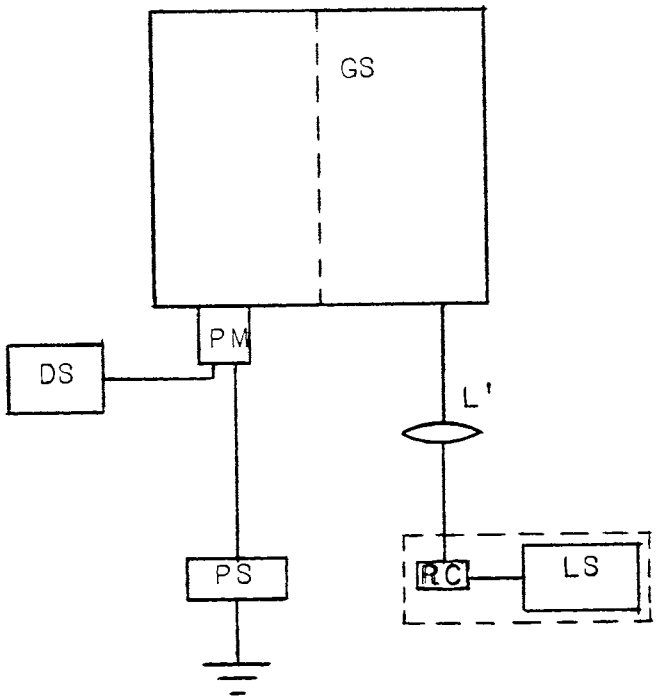

Fig. 1. The laser source LS illuminates the sample in the Raman cell RC. Scattered radiation is conveniently observed at right angles to the exciting radiation and passes into a grating spectrometer GS. Emerging radiation is transduced by a suitably chosen photomultiplier PM into an electrical signal which is then amplified and recorded by the detection system DS. The PM power supply is designated PS.

THE simplest photoelectric technique requires four components (Fig. 1) whose specifications are somewhat interdependent: 1) a laser source. 2) a scattering cell, 3) a spectrometer (or spectrograph). and 4) a detection system.

A typical arrangement (Fig. 2a), utilizing a He-Ne laser (6328A) comprises a laser tube and two resonator mirrors. The output beam is focused by means of a lens into the Raman cell. Before entering the spectrometer slit, the scattered radiation is collected by another lens. Doubling the exciting energy, a third mirror reflects the transmitted beam back through the cell. For measuring depolarization factors the plane of polarization of the laser beam is rotated by means of the polarization rotator. The filter removes incoherent radiation from the output beam.

Since noble gas ion lasers oscillate at many wavelengths, enclosing a prism in the cavity (Fig. 2b) where the prism and resonator mirror form one unit, provides the means of wavelength selection and achieves a monochromatic laser beam.

The Raman cell can be illuminated in various ways. If the laser is focused along the axis of cylindrical cell RC (Fig. 3a) the focal region may be considered an approximate filamentary source of Raman radiation. By aluminizing the rear portion of the cell to yield a cylindrical mirror M, a two-fold gain in light-collecting efficiency is obtained provided reflection losses

are negligible. Incorporating elliptical reflector ER (Fig. 3b) the geometry is such that the focal region inside the Raman cell and the slit of the spectrometer become the foci of the ellipse. Fig. 3c depicts a multiple transversal arrangement in which the laser beam is reflected many times within the Raman cell. It may be desirable to place the Raman cell inside the cavity since there the beam power is very much greater than

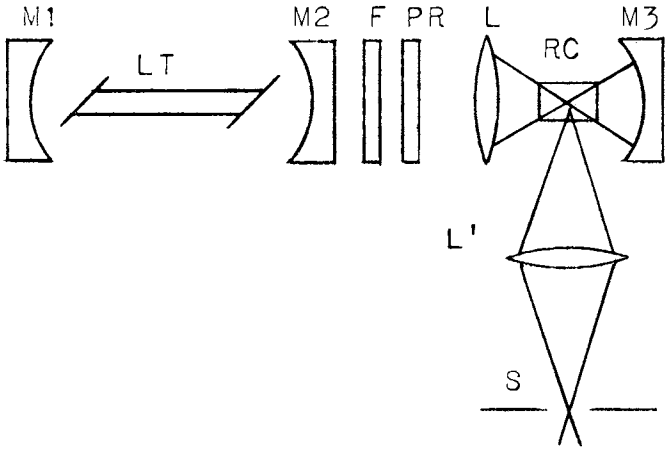

Fig. 2. (a) Typical arrangement of laser-Raman cell combination. LT = laser tube, M1, M2 = laser resonator mirrors, F = filter, PR = polarization rotator, L = laser beam focusing lens, RC = Raman cell, M3 = laser beam feed back mirror to enhance illumination of sample, L' = transfer optics, S = entrance slit of spectrograph or spectrometer.

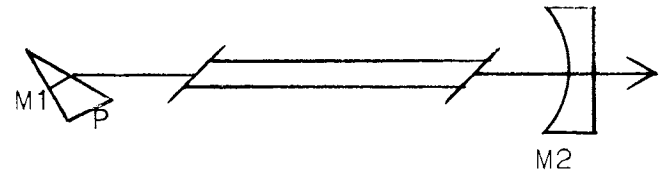

(b) Arrangement for a noble gas ion laser. The wavelength selector prism P and the resonator mirror M1 form one unit.

for the output beam. The single pass Raman cell RC must then be provided with Brewster angle windows (Fig. 3d). If only the vibrational spectra are investigated, the different assemblies are equally well suited for work with liquid (10-14) or gaseous samples. For high resolution Raman spectroscopy of gases the arrangement in 3d was found advantageous (15) with a He-Ne laser as the light source. Additional improvements were achieved by replacing the single pass cell RC with a multiple pass cell (16). With a more powerful argon-ion laser rotational Raman spectra were photoelectrically recorded using the basic system of Fig. 2a (17). For study of transparent crystals the same arrangement has proved workable whereas for opaque solids the reflection method of Fig. 3e was successful (18).

Spectra may be obtained either photographically or photoelectrically. For the study of rotational structure of vibrational Raman bands of polyatomic molecules it has been customary thus far to rely on photographic detection. Plane grating spectrographs possessing large f/numbers and set to high orders to obtain the desired dispersion and resolving power were found necessary to photograph within several tens of hours. To achieve a limiting resolution of 0.05 cm^{-1} a practical resolving power of 316,000 is needed to observe pure rotational Raman spectra excited by the He-Ne 6328A laser line. With a photographic plate resolving power of 50 line

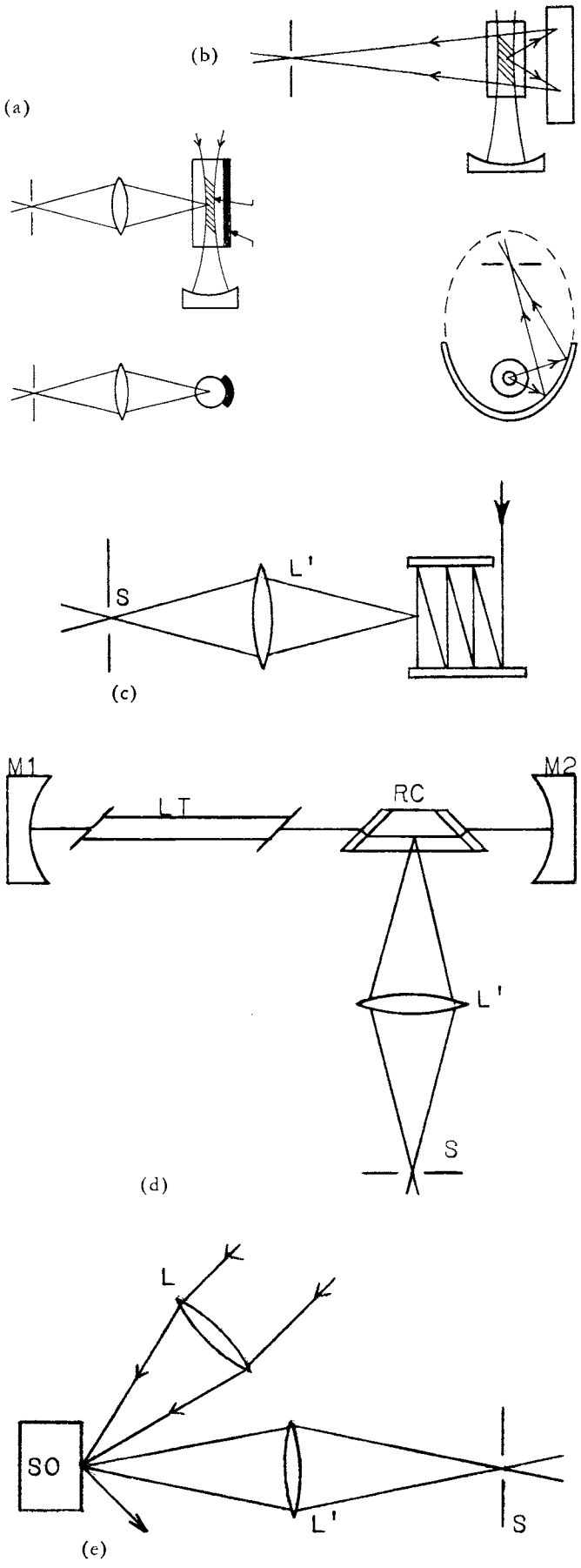

Fig. 3. Several methods of illuminating a Raman cell.

pairs/mm, which is typical of the coarse grain Kodak type 103a-E emulsion, a maximum value for the plate factor is 2.5 cm^{-1}/mm. For a 300 groove/mm plane diffraction grating blazed at 63°28′, operating in the 9th order in Littrow mounting, the requisite focal length of the camera mirror (or lens) is then nearly 2 meters. The largest compatible gratings are 125x254 mm^2 in area, so that the f/number of the camera is then nearly f/14. Under these conditions it is necessary to expose the fast 103a-E plates 20 or more hours to obtain useful spectra (15, 16). With the newer, more sensitive Kodak type Ia-E plates exposure times are reduced by nearly a factor of two.

Despite such emulsion advances photoelectric technique shows greater promise in Raman research and analysis. Commercially available spectrometers are now in wide usage, especially for problems that do not require the utmost in resolution, such as Raman spectroscopy of liquid and solid samples. In both photographic and photoelectric readout, the very strong Rayleigh line has always been a most unwelcome component in the spectrum of scattered radiation. Severe amounts of stray light and grating ghosts originating from Rayleigh radiation have often disrupted the Raman spectrum particularly in the region of small wavenumber shifts. Polarization of the laser beam, however, can be turned to good advantage to block the highly polarized Rayleigh line. By aligning the direction of vibration of the electric vector of the laser with the viewing direction, the Rayleigh line can almost be removed from the spectrum of the scattered radiation. The success of this trick depends on several factors: 1) In the study of liquids composed of anisotropic molecules one finds that the Rayleigh line is flanked by strong, unresolved, rotational wings which are depolarized. These may be sufficiently intense to scatter light and stir up grating ghosts which, in turn, may mask portions of the Raman spectrum near the exciting line. 2) The Q-branches of the totally symmetric vibrations would also be absent from the Raman spectrum, which may not be desirable. If the 459 cm^{-1} line of CCl_4, the 992 cm^{-1} and the 3062 cm^{-1} lines of C_6H_6 are to be observed one cannot then use this method to suppress the Rayleigh line. 3) Laser beam polarization has proved to be a most important parameter in the assignment of Raman spectra of crystals and it may not be desirable to have the observation direction coincide with the vibration direction of the electric vector of the laser radiation.

In experimental requirements where advantage cannot be taken of laser beam polarization to suppress the Rayleigh line, a double spectrometer, equipped with high-efficiency gratings, has been found indispensable. The double dispersion and resolving power, and most importantly, the reduction of stray light to tolerable levels even in the immediate proximity of the exciting line make it a formidable instrument for Raman

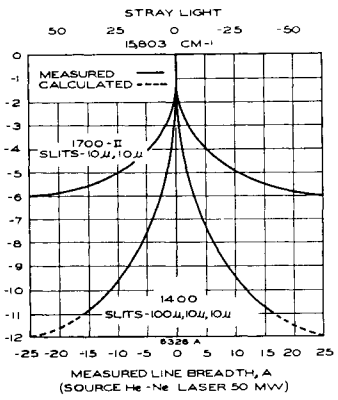

Fig. 4. Stray light levels in single and double spectrometers (from Ref. 18).

spectroscopy. Fig. 4 shows the results of a quantitative study of stray light in a Spex model 1700 (single) and a 1400 (double) spectrometer (19). At 10A away from the He-Ne 6328A line (I_0) scatter is $10^{-5}I_0$ for the 1700 and only $10^{-9}I_0$ for the 1400, with an ultimate drop to $10^{-14}I_0$ beyond 50A. Since the intensities of vibrational Raman bands are $10^{-3}I_0$ or less the value of a double spectrometer cannot be overemphasized.

Here again, a focused laser beam to excite Raman scattering is of great advantage not only in working with small sample volumes but also for maximum efficiency in collecting the scattered light. With a lens essentially free of aberrations, absorption and reflection losses, the full output power of a laser can be concentrated into a diffraction limited focal volume. For ease of computation, this may be assumed to be that of a right circular cylinder of height h and diameter d. With conventional (i.e., mode unstabilized) lasers diameters of 10μ are easily achieved. If the light collection system (lens L′ of Figs. 2 and 3) is also free of aberrations, absorption and reflection losses and forms an image of the source (the focal volume = effective scattering volume of the sample) on the spectrometer slit S, the fundamental relation of radiometry, applies. That is, the radiance of the source is equal to the radiance of the image (radiance = radiant flux per unit solid angle per unit projected area). This yields the simple relation $\Omega = m^2\Omega_0$ where Ω_0 is the solid angle of the spectrometer collimator, m is the magnification of the lens L′ when it forms the image of the source on the slit, and Ω is the solid angle subtended by the lens L′ at the source. On the basis of these considerations Benedek and Fritsch (20) have shown that for optimum collection of the Raman scatter the focal length f of the condensing lens L (See Fig. 2a) is to be chosen according to the relation $(f/a) = w/m\lambda)$ where a is the diameter of the incident laser beam, w is the width of the spectrometer entrance slit, λ is the wavelength of the laser radiation and the magnification m is given by $m = 3w^2/\lambda h'$ where h′ is the height of the spectrometer entrance slit. The focal length f′ of the lens L′ is such that the source and slit are at conjugate positions. A very substantial increase in the amount of light collected is thus achieved.

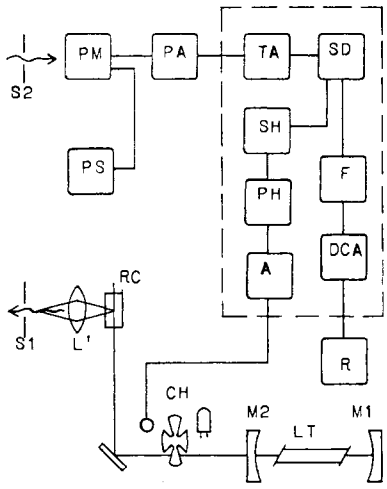

Fig. 5. Schematic of a lock-in detection system. PA = preamplifier, TA = tuned amplifier (tuned to chopping frequency f_0), SD = synchronous detector, F = filter, DCA = DC amplifier, R = recorder. The reference signal and the Raman excitation are modulated at frequency f_0 by a mechanical chopper CH. A = amplifier, PS = phase shifter, SH = shaper, S_1, S_2 = entrance and exit slits of monochromator. The components contained in the dashed outline comprise the lock-in amplifier. Other symbols are as defined in Fig. 2.

SEVERAL detection systems have been proposed to amplify the weak signals generated by a photomultiplier tube before a stripchart recording can be obtained. Since all PM tubes are sources of noise, special attention must be given to distinguishing the genuine signal from the noise and ultimately recording the signal only. The method of synchronous (lock-in), amplification (Fig. 5) is now widely employed in preference to a straight DC method. If a sample in the Raman cell RC is illuminated with radiation of constant intensity, the PM produces a DC signal resulting from the radiation transmitted by the spectrometer along with any noise developed within the PM.

Cooling, of course, is the first step in diminishing the latter. The noise spectrum of the PM is frequency-dependent so that with DC amplification the genuine signal and the background will be equally amplified, there being then no improvement in the signal to noise (S/N) ratio. In synchronous detection, selective amplification is accomplished by modulating the excitation of the Raman scattering at a frequency f_0 (usually several hundred cycles per second) at which the noise spectrum of the PM has small amplitude. AC amplification of the genuine signal at the frequency $f_0 \pm \Delta f$, where Δf is the band-width of the amplifier, brings the signal to a sufficiently high level upon subsequent rectification to drive a stripchart recorder R. The AC amplifier output is fed into a synchronous detector, tuned and phase locked to the modulation frequency f_0 through a reference signal generated independently but synchronously with the excitation of the Raman scattering. Since the amplifier has a finite, though narrow, band-width Δf, noise which occurs at $f_0 \pm \Delta f$ is also amplified. But with modern lock-in amplifiers Δf is so small that a significant improvement in S/N results.

Currently favored in many laboratories is another method of distinguishing weak Raman signals from noise. Called photon counting, it is similar in principle to pulse counting long familiar in x-ray and gamma ray intensity measurements. When a photon impinges on the cathode of a photomultiplier, the photoelectron that is released is accelerated to the first dynode positively charged to 100 volts or so. Secondary electrons released at this dynode are then accelerated to the next dynode where further electrons are released. By the time this procedure is repeated 10-13 times in the dynode chain of a typical photomultiplier, the initial electron winds up as a burst of perhaps 10^6 electrons. The height or intensity of the pulses varies from one signal photon to the next. Each photon thus contributes differently to the signal current, the intensity range of which extends over about an order of magnitude.

On the other hand a good deal of the noise hovers below the signal range. When a "noise" electron originates down the dynode chain, its resultant amplified pulse will be progressively smaller on the average than that from a "signal" electron. Only those "noise" pulses originating at the cathode will have a height equal to pulses from a photon. Theoretically, then, much of the thermal noise can be isolated and discriminated against with a suitable low-pulse-blocking circuit. At the high energy end, pulses originate from another source of noise: cosmic rays and radioactivity, the latter largely from K_{40}, a component in natural potassium and a common glass and quartz impurity.

By interspersing an energy "window"—variable low and high-intensity blocking circuitry—a real gain in signal: noise is made possible (Fig. 6). The magnitude of this gain depends on individual photomultipliers—the dark emission count of which may vary over many decades—and the temperature of the tube. Photon counting often obviates the need for cooling, although for ultimate performance both are often coupled.

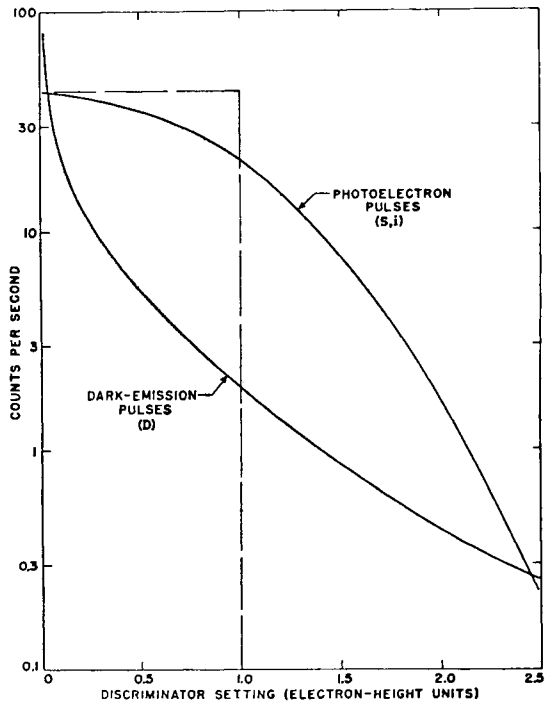

Courtesy W. A. Hiltner, Astronomical Techniques, (*U. of Chicago Press,* 1962)

Fig. 6. Noise pulse spectrum of a photomultiplier (schematic).

To record data from pulse counting electronics on a conventional stripchart recorder, a delay line (pulse shaper PS) first broadens the pulses. These are then integrated with a variable time constant circuit, the resultant current from which is then amplified and recorded.

Photon counting has proved to be superior to lock-in and straight DC amplification for signals of low light levels, a characteristic of all Raman lines. For strong signals, photon counting is limited by the time resolution of the pulse amplifier and discriminator.

To reject the noise produced by electronic components, Arrecchi *et al* (20) have just announced a variation which automatically subtracts the noise pulses originating within the electronics from the total pulses. A mechanical chopper modulates the excitation radiation in the manner shown in Fig. 5. During the "open" time of the chopper the photomultiplier output consists of signal + noise pulses whereas during the "closed" time of the chopper the photomultiplier output contains only noise pulses. The "signal + noise" and the "noise only" pulses are sent alternately to a bidirectional digital counter. An electronic gate and switch are operated synchronously with the excitation of the Raman scattering and thus control the add and subtract operations of the counter.

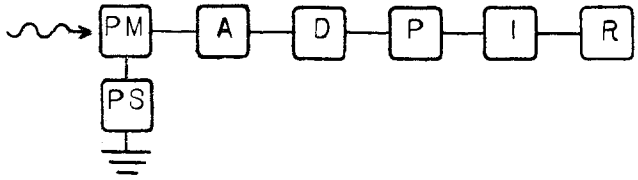

Fig. 7. Schematic of a simple photon counting system. A = amplifier, D = discriminator, P = pulse shaper (delay line), I = integrator, R = recorder.

A third method developed for detection of weak light signals is that of "intensity correlation" (22-25). Radiation is received by two detectors (photomultipliers) whose output is then correlated (see Fig. 8) and recorded after suitable amplification. Here there are statistical fluctuations in a light beam and a mathematical relationship exists between these fluctuations and the spectrum. The Raman radiation RS is analyzed by a spectrometer GS, whose output consists of a narrow band of radiation of frequency $\nu \pm \Delta\nu$. Two independent photomultipliers PM1 and PM2 convert the intensities incident upon them into voltages which are then multiplied and integrated in an electronic correlator circuit. A variation of the arrangement (Fig. 8b) requires only one photodetector, the output of which is correlated in a manner similar to that given in Fig. 8a. These are somewhat similar in principle to a Michelson interferometer, where beam amplitudes rather than beam intensities are correlated. The method has been applied to Raman spectroscopy by Pao *et al.*, (23) who, however, omitted a delay line in their system which would serve to obtain information about the coherence of the radiation and thus the line widths.

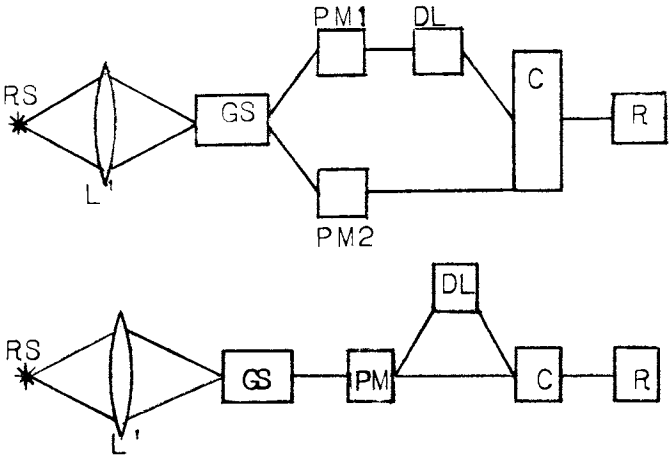

Fig. 8. Schematic of an intensity correlation system. RS = source of Raman radiation, GS = spectrometer, PM = photomultiplier, DL = delay line, C = correlator (multiplier and integrator), R = recorder.

THE role of Raman spectroscopy in quantitative molecular structure studies has been exemplified for gaseous substances by several investigators (6, 7, 8). For instance, one may cite the ethane molecule structure, studied for many years by several methods including infrared spectroscopy. The question of whether the two methyl groups are posed in a staggered or eclipsed relative conformation at equilibrium has been answered mostly by compiling results of different experimental techniques. The eclipsed model is of point group D_{3h} whereas the staggered model is of point group D_{3d}. The different selection rules for the Raman active degenerate vibrations permit, at once, a unique and unambiguous resolution of this structural problem. Thus, for the D_{3h} model the selection rules for the quantum number K for the rotational transitions of the E″ vibrations are $\Delta K = \pm 1$ while for the corresponding E_g vibrations of the D_{3d} model they are $\Delta K = \pm 1, \pm 2$. The E′ vibrations of the D_{3h} model also have the selection rules $\Delta K = \pm 1$ whereas the corresponding E_u vibrations of the D_{3d} model are Raman inactive. Thus, by simply noting whether or not there are two series of Q-branches (for $\Delta K = \pm 1, \pm 2$) in the degenerate Raman bands, the problem of the eclipsed *vs.* the staggered model is solved (26, 27). A further difficulty concerned the value of the moment of inertia about the axis joining the two methyl groups (C-C bond). Infrared spectral data were found to be in conflict with those of independent Raman investigations. A careful study of the methods of obtaining experimental data resolved this difficulty (28), too. The bond lengths and interbond angles that can now be calculated from a combined treatment of infrared and Raman spectroscopic data are fully consistent with the results obtained from the electron diffraction technique and the more precise method of microwave spectroscopy.

It is a well-known fact that the wavenumbers of molecular vibrations are not the same for liquid and gaseous states of aggregation of a substance. Investigations of the vibrational Raman spectrum of compressed hydrogen indicate that increased densities of the gas cause frequency shifts and broadenings of the Q-branch lines of the fundamental vibration. The shifts are interpreted as vibrational perturbations whereas the broadening is ascribed to effects of intermolecular forces (29).

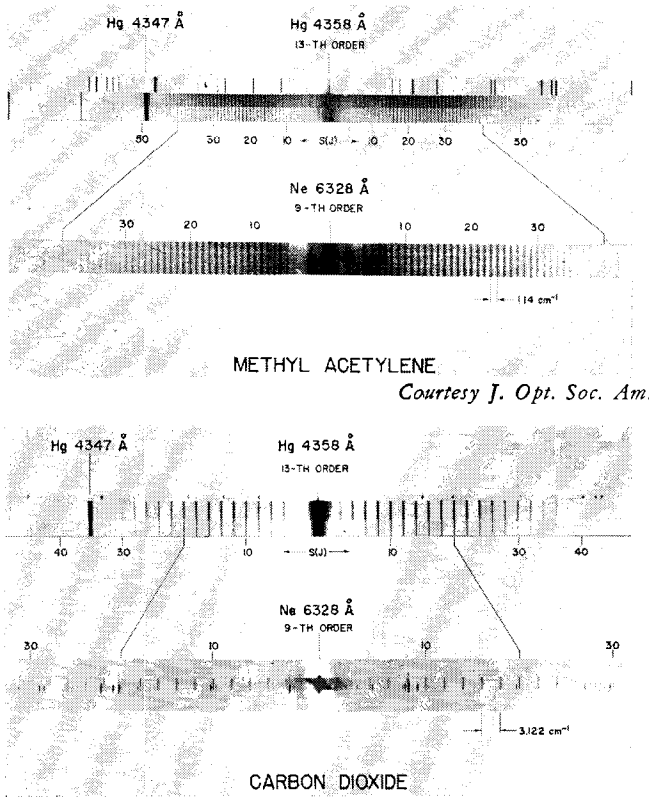

Courtesy J. Opt. Soc. Am.

Fig. 9. Pure rotational Raman spectra of methyl acetylene and carbon dioxide at atmospheric pressure, photographed with a large plane grating spectrograph. The methyl acetylene spectra were obtained in 14 hours of exposure on Kodak 103a-O plates (Hg-arc excitation) and in 33 hours of exposure on Kodak 103a-E plates (He-Ne laser excitation, with multiple pass Raman cell). The carbon dioxide spectra were obtained in 4 hours (Kodak 103a-O plate, Hg-arc excitation) and 35 hours (Kodak 103a-E plate, He-Ne laser excitation with a single pass Raman cell and cylindrical lens placed in front of the photographic plate). (See Refs. 14, 15.)

Applying laser sources to excite Raman spectra of low pressure gases has been successfully demonstrated by Weber, Porto and their coworkers (15-17, 30). Figure 9 shows the pure rotational Raman spectra of methyl acetylene and carbon dioxide gas at 760 torr photographed on Kodak 103a-E plates under high resolution in 33 hours and 35 hours respectively. A He-Ne laser and a multiple traversal Raman tube (Fig. 10) were used (14, 15) for methyl acetylene. For comparison, the Hg arc excited spectra were obtained in 14 hours and 4 hours, respectively. Photoelectric recording of Raman spectra of

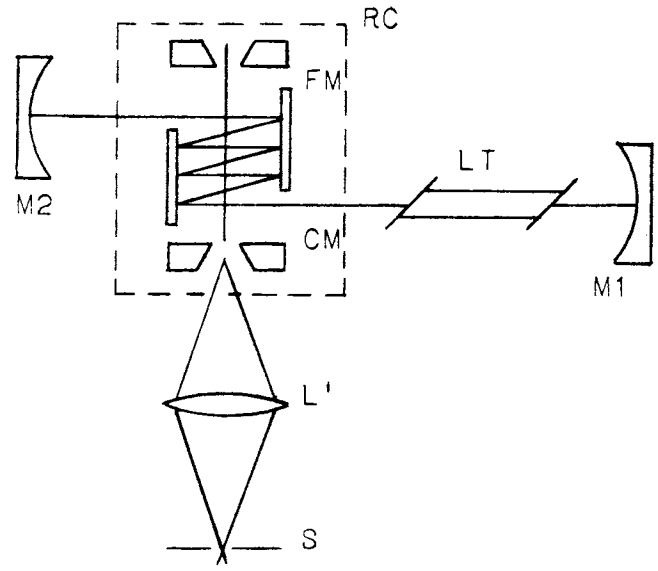

Fig. 10. Schematic of a laser Raman excitation system with a multiple traversal Raman cell inside the laser cavity.

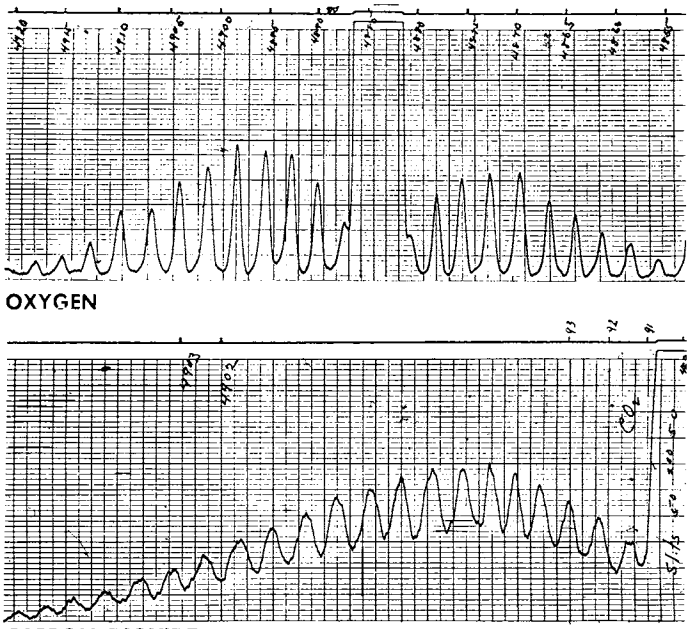

Fig. 11. Photoelectrically recorded pure rotational Raman spectra of oxygen and carbon dioxide (Stokes side only). The spectra were obtained at atmospheric pressure, with a Spex model 1400 double spectrometer and lock-in detection system. An argon laser ($\lambda = 4880$A) provided the excitation radiation. The Stokes side is to the left. (Courtesy of Dr. S. P. S. Porto.)

gases has been similarly demonstrated (17, 30). Fig. 11 shows the photoelectrically recorded pure rotational Raman spectra of CO_2 and O_2 from a Spex model 1400 double spectrometer and lock-in detection system. The exciting source was an argon-ion laser with output powers of around 200-300 mW in the 4881A and 5145A lines.

All properties possessed by a laser beam have not yet been fully exploited. Thus, to achieve a limiting resolution of 0.05 cm^{-1} in a Raman spectrum several factors, besides the resolving power of the spectrograph, must be considered. For example, for a gas at room temperature Doppler broadening of the Raman lines is by no means negligible. The Doppler width $\Delta\sigma_{1/2}$ (full width at half intensity) of a spectrum line of wavenumber σ_0 is given by $(\Delta\sigma_{1/2}/\sigma_0) = 7.16\text{x}10^{-7}(T/M)^{1/2}$ where T is the absolute temperature and M is the molecular weight. For the He-Ne 6328A laser line $\sigma_0 = 15{,}800$ cm^{-1} so that at room temperature (T=300°K) the Doppler widths for the Raman lines of ethane (M=18) and benzene (M=78) are then 0.046 cm^{-1} and 0.022 cm^{-1}, respectively. Other causes of line broadening are due to pressure. For simple non-polar gases (O_2, N_2, CO_2) the pressure broadening coefficient of Raman line widths for the case of the anisotropic scattering (rotational structure of Raman bands) has been measured to be of the order of $5\text{x}10^{-2}cm^{-1}$/atm for O_2 and N_2, and $12\text{x}10^{-2}cm^{-1}$/atm for CO_2. Furthermore, the broadening effects are not constant but are dependent on the rotational state of the molecule (31). For polar gases the broadening coefficient is of the order of 1 cm^{-1}/atm (6). The observed widths of the Raman transitions (rotational Raman lines) are then the result of a complicated convolution of the natural line width with the line profiles ascribable to other causes (Doppler effect, pressure broadening, width of exciting line, apparatus width etc).

Work is in progress to minimize the various factors that contribute to Raman line broadenings. Among the information that would become available through narrower line widths is the resolution of the K-structure of the rotational Raman transitions in symmetric top molecules with $\Delta J = \pm 1, \pm 2$. This would yield data on the centrifugal distortion constants which are very difficult to determine accurately; also the fine structure of degenerate bands provide improved rotational constants, Coriolis constants, and centrifugal distortion constants for excited vibrational states. The contrast between the potential of high resolution Raman spectroscopy with a laser and with the best other practical light source available heretofore, namely the water-cooled low-pressure Hg arc, is amply illustrated in Fig. 12 which shows the structure of the blue mercury line at 4358A (32). The width of the central intense and asymmetric portion is at best 0.20 cm^{-1}; practical non-stabilized He-Ne lasers operating in multimode emit the 6328A radiation with a width less than 0.05 cm^{-1}.

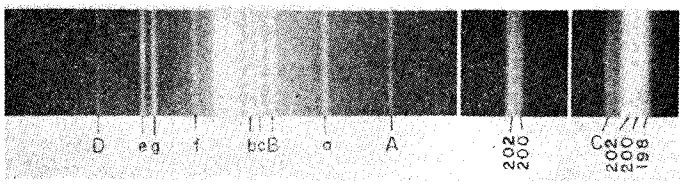

Courtesy J. Opt. Soc. Am.

Fig. 12. Hyperfine structure of the blue ($\lambda = 4358$A) mercury line used heretofore to excite Raman spectra (from Ref. 32).

It is in the study of crystalline solids that the Raman effect really shines since this scattering results from the interaction of radiation with lattice vibrations (phonons). The complementary nature of Raman effect and infrared absorption applies here just as it does to individual molecules. One distinguishes between the first order Raman spectrum due to the creation or annihilation of single optical phonons (Stokes and anti-Stokes scattering, respectively) and the second order Raman spectrum from scattering processes involving pairs of phonons. The first and second order of Raman effect in crystals is analogous to the fundamental frequencies of vibrations and the overtone and combination vibrations in the spectrum of a molecule with an intensity ratio of first to second order process of about 1000:1 providing both processes are allowed by the selection rules. Prior to the availability of laser sources the state of knowledge of the Raman effect in crystals was utterly confused, with widely differing results reported for the components of the polarizability tensor. And the impedi-

ments were strictly the result of the ill defined state (i.e., beam collimation and polarization) of the exciting radiation. The great impact of laser sources on Raman spectroscopy of crystals can be exemplified by calcite which had been studied extensively with the traditional Hg arc.

Porto *et al* (33) just reexamined the Raman spectrum of calcite with a 50 mw He-Ne laser and a Spex model 1400 double spectrometer followed by a lock-in detection system (see Fig. 2a, with or without lens L but without mirror M3, and Fig. 5). The point symmetry for calcite is D_{3d} and thus the Raman spectrum contains five active vibrations. One vibration is of A_{1g} character and describes the totally symmetric breathing vibration of the carbonate ion. The intensity of this vibration in the Raman effect is determined by non-vanishing components $\alpha_{xx}=\alpha_{yy}$ and α_{zz} of the polarizability tensor. The other four vibrations have symmetry character E_g with non-vanishing tensor components $\alpha_{xz}=\alpha_{yz}$ and/or $\alpha_{xx}=\alpha_{xy}=-\alpha_{yy}$. Two of these have been assigned to the internal vibrations of the carbonate ion and the remaining two are due to external or lattice vibrations.

Previous observations of the Hg arc excited Raman spectrum yielded ambiguous results for the polarization of the strong A_{1g} mode at 1088 cm^{-1}. They take the form of a non-vanishing component α_{xy} forbidden by the selection rules for the A_{1g} mode. With a cartesian coordinate system xyz fixed in the crystal and defined such that the z- and y- axes represent the trigonal (optic) axis and a binary axis, respectively, the apparent value of α_{xy} was found to be small or negligible in comparison to α_{xx} when the directions of the incident and scattered light are in the xy-plane, or in the yz plane but removed from the optic axis. On the other hand, the apparent value of α_{xy} was found to be high when either the incident or scattered light is directed along the optic axis.

Well defined states of collimation and of polarization of the laser beam may be observed in the Raman spectrum in Fig. 13. The symbols inside the parenthesis indicate, left to right, the polarization of the incident and scattered light while the ones to the left and right outside the parenthesis are the propagation directions of the incident and scattered light respectively. Thus, Fig. 13a is the spectrum when the crystal is illuminated along the z-axis with the laser beam polarized in the x-direction, and the x-polarized scattered light is collected in the y-direction. The resulting $z(\alpha^2_{xx})y$ spectrum reveals all the A_{1g} and E_g vibrations as expected (four vibrations are spanned in the figure; the fifth occurs at 1432 cm^{-1}). The $y(\alpha^2_{xy})x$ spectrum (Fig. 13b) includes all the E_g lines but no detectable A_{1g} scattering. In the $y(\alpha^2_{zz})x$ spectrum (Fig. 13c) only the A_{1g} scattering was detected whereas the $x(\alpha^2_{zx})y$ spectrum (Fig. 13d) reveals all the E_g vibrations but no detectable A_{1g} scattering. These experiments prove that the observed Raman spectrum of calcite is fully consistent with the Raman selection rules based on the D_{3h} point group selection rules and that all previously noted anomalies in the spectrum can be explained by depolarization of the highly convergent incident (Hg-radiation) and scattered light required in the earlier experiments. Further work by Porto and his co-workers on cadmium sulfide (34) zinc oxide (35, 36, 37) iron sulfide FeF_2 (38), F-centers in alkali halides (39), and quartz (40); by Russell (41) and co-workers on silicon (42), gallium phosphide (43), calcium fluoride (44), and calcium tungstate (45) demonstrate the fantastic impact that the laser has had on the field of Raman spectroscopy of crystals. Loudon (46) has given a thorough review of this rapidly moving field. It is not at all unlikely that the boom Raman spectroscopy experienced during the early 1930s will be repeating itself now that well engineered laser sources, spectrometers and completely packaged Raman spectrometric systems are commercially available.

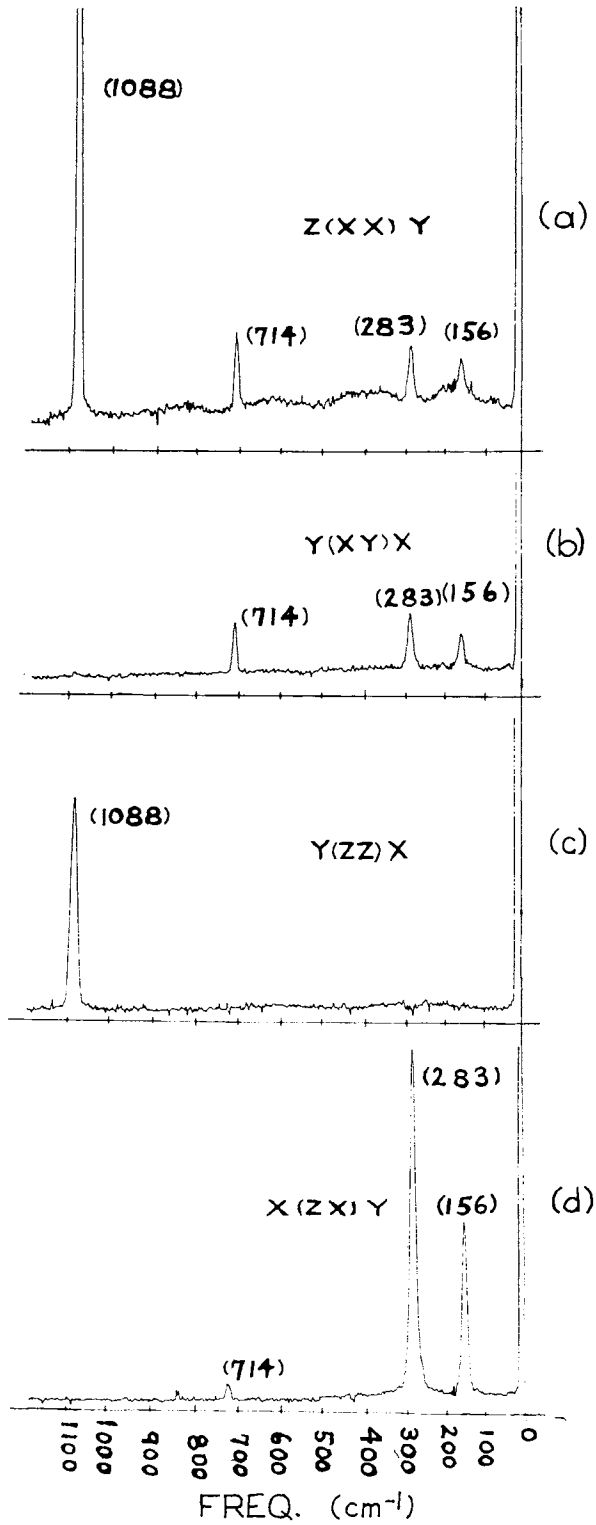

Courtesy Physical Review

Fig. 13. The Raman spectrum of calcite excited by $\lambda = 6328A$ laser radiation shown for various directions of propagation as well as polarization of the incident and scattered light (from Ref. 33).

Acknowledgment

Helpful discussions with Dr. S. P. S. Porto of the Bell Telephone Laboratories are gratefully acknowledged.

REFERENCES

1—C. V. Raman, Ind. J. Phys. 2, 387 (1928).

2—J. Brandmuller and H. Moser, Einfuhrung in die Ramanspektroskopie (Dr. Dietrich Steinkopf Verlag, Darmstadt, 1962).

3—G. Placzek, Rayleigh Streuung und Raman Effekt, in Handbuch der Radiologie, vol. VI, part II, pp. 205 (Akademische Verlagsgesellschaft, Leipzig, 1934). English translation by A. Werbin, U.C.R.L. Translation No. 526 (L).

4—J. R. Nielsen and N. E. Ward, J. Chem. Phys. **10**, 81 (1942).

5—J. Cabannes and A. Rousset, J. Phys. Radium **1**, 155, 181, 210 (1940).

6—H. L. Welsh, E. . Stansbury, J. Romanko and T. Feldman, J. Opt. Soc. Am. **45**, 338 (1955).

7—B. P. Stoicheff, in **Advances in Spectroscopy I**, H. W. Thompson, ed. (Interscence Publishers, Inc., New York, 1959), pp. 91-174.

8—B. P. Stoicheff, in **Experimental Physics: Molecular Physics**, D. Williams, ed. (Academic Press, Inc., New York, 1962), vol. 3, pp. 111-155.

9—S. P. S. Porto and D. L. Wood, J. Opt. Soc. **52**, 251 (1962).

10—R. C. C. Leite, R. S. Moore, S. P. S. Porto, and J. E. Ripper, Phys. Rev. Letters **14**, 7 (1965).

11—T. C. Damen, R. C. C. Leite and S. P. S. Porto, Phys. Rev. Letters **14**, 9 (1965).

12—H. Kogelnik and S. P. S. Porto, J. Opt. Soc. Am. **53**, 1446 (1963).

13—R. C. C. Leite and S. P. S. Porto, J. Opt. Soc. Am. **54**, 981 (1964). S. P. S. Porto, Ann. N. Y. Acad. Sci. **122**, 643 (1965).

14—J. A. Koningstein and R. G. Smith, J. Otp. Soc. Am. **54**, 1061 (1964).

15—A. Weber and S. P. S. Porto, Bull. Am. Phys. Soc. 9, 625 (1964). J. Opt. Soc. Am. **55**, 1033 (1965).

16—A. Weber and S. P. S. Porto, Bull. Am. Phys. Soc. **10**, 101 (1965).

17—S. P. S. Porto, L. E. Cheesman, A. Weber, and J. J. Barrett, J. Opt. Soc. Am. **56**, 551A (1966).

18—J. P. Russell, J. Phys. Radium 26, 620 (1965).

19—D. O. Landon, private communication.

20—G. B. Benedek and K. Fritsch, Phys. Rev. **149**, 647 (1966).

21—F. T. Arecchi, E. Gatti and A. Sona, Rev. Sci. Instr. **37**, 942 (1966).

22—E. Wolf, Jap. J. Appl. Phys. **4**, Suppl. I, 1 (1964).

23—Yo-Han Pao, R. N. Zitter and J. E. Griffiths, J. Opt. Soc. Am. **56**, 1133 (1966).

24—A. L. Fetter, Phys. Rev. **139**, A1616 (1965).

25—M. L. Goldberger, H. W. Lewis and K. M. Watson, Phys. Rev. **142**, 25 (1966).

26—D. W. Lepard, D. M. C. Sweeney and H. L. Welsh, Can. J. Phys. **40**, 1567 (1962).

27—D. W. Lepard, D. E. Shaw, and H. L. Welsh, Can J. Phys. **44**, 2353 (1966).

28—D. E. Shaw, D. W. Lepard and H. L. Welsh, J. Chem. Phys. **42**, 3736 (1965).

29—A. D. May, G. Varghese, J. C. Stryland and H. L. Welsh, Can. J. Phys. **42**, 1058 (1964).

30—A. Weber, S. P. S. Porto, L. S. Cheesman, and J. J. Barrett, J. Opt. Soc. Am. (in print).

31—K. S. Jammu, G. E. St. John and H. L. Welsh, Can. J. Phys. **44**, 797 (1966).

32—D. H. Rank, G. Skorinko, D. P. Eastman, G. D. Saksena, T. K. McCubbin, Jr., and T. A. Wiggins, J. Opt. Soc. Am. **50**, 1045 (1960).

33—S. P. S. Porto, J. A. Giordmaine and T. C. Damen, Phys. Rev. **147**, 608 (1966).

34—B. Tell, T. C. Damen and S. P. S. Porto, Phys. Rev. **144**, 771 (1966).

35—S. P. S. Porto, B. Tell and T. C. Damen, Phys. Rev. Letters **16**, 450 (1966).

36—T. C. Damen, S. P. S. Porto and B. Tell, Phys. Rev. **142**, 570 (1966).

37—R. C. C. Leite and S. P. S. Porto, Phys. Rev. Letters **17**, 10 (1966).

38—P. A. Fleury, S. P. S. Porto, L. E. Cheesman and H. J. Guggenheim, Phys. Rev. Letters **17**, 84 (1966).

39—J. M. Worlock and S. P. S. Porto, Phys. Rev. Letters **15**, 697 (1965).

40—S. P. S. Porto, private communication.

41—J. P. Russell, Journal de phys. **26**, 620 (1965).

42—J. P. Russell, Appl. Phys. Letters **6**, 223 (1965).

43—H. V. Hobden and J. P. Russell, Physics Letters **13**, 39 (1964).

44—J. P. Russell, Proc. Phys. Soc. **85**, 194 (1965).

45—J. P. Russell and R. Loudon, Proc. Phys. Soc. **85**, 1029 (1965).

46—R. Loudon, Advances in Physics **13**, 423 (1964).

SPEX DOUBLE MONOCHROMATOR

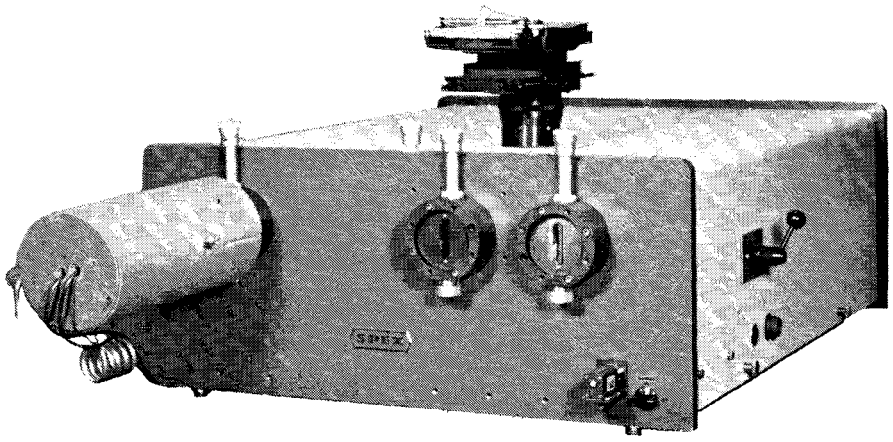

MODEL 1400

Scattered Light

10^{-11} of exciting laser line at $50cm^{-1}$ distance, dropping ultimately to 10^{-14} beyond $100cm^{-1}$, achieved through pair of Bausch & Lomb gratings.

Grating Blaze Efficiency

Typically 70-80% compared with 40-50% for non-B&L gratings. Result: a double spectrometer with twice to four times the optical speed otherwise attainable.

Throughput and Resolution

Double dispersion is achieved by reversing direction thus adding the dispersion of each grating. This achieves twice the resolution if slit widths are set identically or twice the luminosity if slit widths are set to equal bandpass.

Minimal Optical Losses

8 reflectors including gratings.

ER-3 PHOTON COUNTING/DIRECT CURRENT ELECTRONIC READOUT

Designed for detection of extremely low-level photomultiplier signals such as those from Raman spectra, this system contains both pulse counting and direct current amplification which can be applied alternatively. Pulse counting is considered unsurpassed for separating signal from noise which originates in the photomultiplier and its attendant circuitry rather than in the source of radiation. Ideal for the detection of extremely faint signals, photon counting (pulse counting of light quanta) fails when the event rate exceeds the system's counting capability. At such signal levels the ER-3's high-performance dc amplification section may be switched into operation. Either amplifier output is then fed into a fast-sweep stripchart recorder which also includes a separate event marker pen for indicating uniform wavelength intervals.

Also enclosed in the 48" high, standard 19" rack-panel is a power supply for the photomultiplier and controls for the 1513 wavelength scanning drive of the spectrometer. The photon counting components conform to USAEC Standard Nuclear Instrument Committee specifications (TID-20893) which permit the electrical and mechanical addition and interchange of other plug-in modules. Blank panel spaces are available for this purpose to accommodate up to six additional modules 1.35" wide by 9.797" deep by 8.719" high, or a smaller number of wider modules.

PHOTON COUNTING

This section consists of: 1) an RC amplifier which amplifies and shapes the photon and noise pulses originating from the photomultiplier so they can be separated by 2) a single channel pulse-height analyzer with continuous control of the lower (E) and upper (ΔE) levels of discrimination; 3) a log/linear precision ratemeter which integrates the pulses to provide a suitable signal to 4) a stripchart recorder.

ER-3 SPECIFICATIONS

1) RC Linear Amplifier

INPUT

Rise time: 50-250 nsec
Source Impedance: <500 ohms

OUTPUT

Rise time: 100-700 nsec
Shaping: 1 μsec, double RC clipped
Range: 0-10v
Gain: Adjustable 20-1200X
Overload: Complete recovery to baseline within 20 μsec from 100X overload
Count rate: Maximum greater than 100k pps

2) Pulse-Height Analyzer

E DISCRIMINATOR (Lower Level)

Range: 200 mV to 10 V
Linearity: ±0.25% of dial setting

ΔE DISCRIMINATOR (Upper Level)

Range: 0-10 V
Window stability: 0.5 mV/°C
Count rate: Stable to 500k pps
Output amplitude: 10 V into 1000 ohms
Output pulse width: 500 nsec

3) Log/Linear Precision Ratemeter

Sensitivity: Adjustable with 10-turn pot from 0.25 to reduce noise pickup from pulse-height analyzer
Linearity: 0.5%
Input count rate: to 100k pps
Recorder output: 0-10 mV, 0.5% linearity
Linear count rate: 13 ranges from 10 to 100,000 cps full scale
Log count rate two 3-decade ranges
Internal calibration: test signals 10, 100, 1,000 and 100,000 pps
Time constants: 0.25, 0.4, 1, 2, 4, 10, 20, and 40 sec

4) Stripchart Recorder

Range: 0-10 mV full scale
Response time: 0.4 sec
Span: 10 inches
Wavelength marker: Separate event pen
Chart speed: adjustable

DC AMPLIFICATION, PICOAMMETER

Sensitivity: 10^{-11} to 10^{-3} amp full scale in decade ranges
Bucking current: 10^{-9} to 10^{-3} amp full scale
Time constant: Variable 0.1 to 30 sec in 6 steps
Accuracy: 1% on all ranges, readout on 6" meter

PHOTOMULTIPLIER POWER SUPPLY

Range: 0-2000V in 1 V increments
Max. Current: 10 mA
Regulation: 0.0025%
Overload: Protective circuit interrupts high-voltage if current exceeds 11 mA

DIMENSIONS AND UTILITIES

All components fit a standard 19" rack panel 48" high and 22" deep.

Power: 115 v, 50 or 60 Hz (specify)

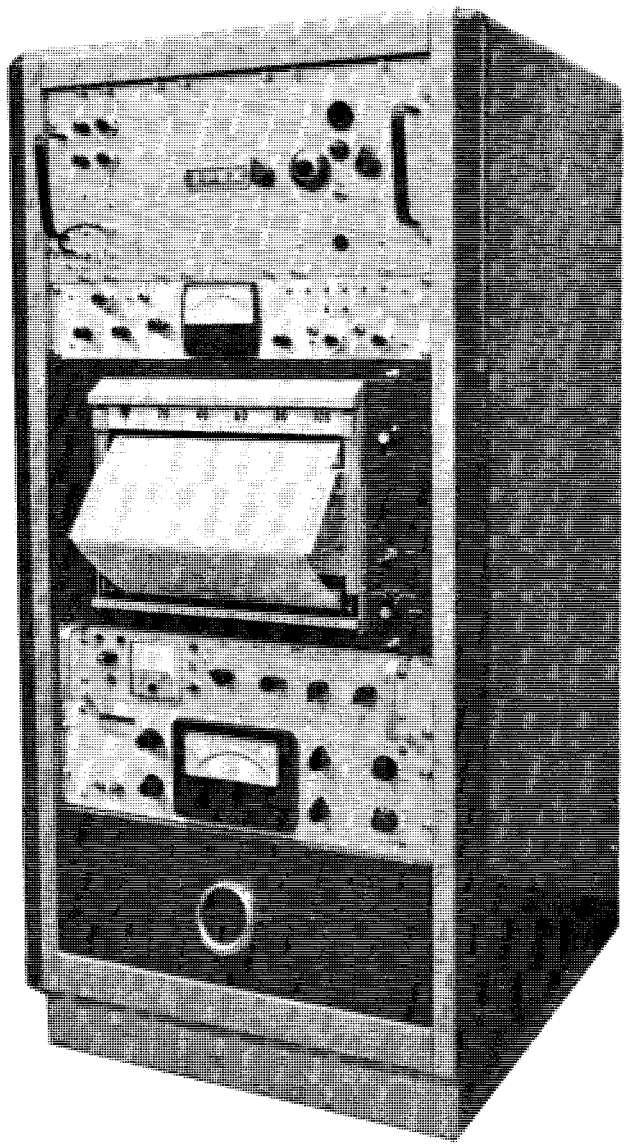

ER-3 PHOTON COUNTING/DIRECT CURRENT ELECTRONIC READOUT $7,155.00

S A S JOURNAL AWARD

Professors J. B. Urenovich, A. G. McDiarmid and E. R. Nixon of Pennsylvania State University shared the 1965 Journal Award for their paper, "Infrared and Raman Spectra of Some Penta-Methyldisilanyl Compounds." Presented to Dr. Urenovitch at the Fifth National Meeting of the Society for Applied Spectroscopy, the annual award is sponsored by Spex Industries, Inc., for the best paper published in **Applied Spectroscopy** as judged by the Journal Award Committee, chaired, for Volume 19 by J. S. Ziomek.

A. J. Mitteldorf (right) presents the 1965 Journal Award to Dr. J. B. Urenovitch, Air Products and Chemicals Co.